Mutations in the *RACGAP1* gene cause autosomal recessive congenital dyserythropoietic anemia type III

Congenital dyserythropoietic anemia type III (CDA III) is one of the rarest types of CDA. The autosomal dominant form of CDA III, is due to mono-allelic mutations in the *KIF23* gene (MIM:105600); two such mutations described so far in a total of three families.[1,2] *KIF23* encodes mitotic kinesin-like protein (MKLP1), which dimerizes and combines with a homodimer of the RACGAP1 protein (Rac GTPase-activating protein 1), to form the centralspindlin complex regulating Rho GTPase activity and required for cytokinesis.[3,4] Sporadic cases with CDA III pathology have been reported, suggesting a different genetic alteration.[5] All reported CDA III cases present with a core phenotype consisting of variable degree of macrocytic anemia, signs of intravascular hemolysis, and giant multinucleated erythroblasts in the bone marrow. Additional symptoms such as multiple myeloma, monoclonal gammopathy, angioid streaks, hemosiderinuria, hepatosplenomegaly, iron overload or cirrhosis were described in some CDA III patients.[6-9] Using next generation sequencing (NGS) in combination with *ex vivo* erythroid differentiation we identified two pathogenic missense mutations in the *RACGAP1* gene in three unrelated families affected with the recessive form of CDA III.

Written informed consent was obtained for all participants in this study that was conducted in accordance with the Declaration of Helsinki's ethical principles, and the protocol was approved by the Ethics Committee associated with the UIC on 04/08/2021.

The first patient is an 18-year-old male (Family A, II.2, Figure 1A) diagnosed at the age of 4 months suffering from severe macrocytic anemia and hepatosplenomegaly. The parents come from a small village in the South of Spain; with a possible common ancestor 11 generations prior to the proband. Peripheral blood and bone marrow showed multiple erythroid abnormalities, including multinucleated erythroblasts (*Online Supplementary Table S1;* Figure 1B*; Online Supplementary Figure S1A* to *H*). At 18 months of age, radiography of the skull showed a hair-on-end appearance and a computed tomography scan revealed widening of the diploic space (data not shown), both characteristic features of chronic hemolytic disease with ineffective erythropoiesis. Hemolysis was confirmed by increased plasma bilirubin, lactate dehydrogenase (LDH) and undetectable haptoglobin. Serum ferritin levels are normal at 18 years of age and iron overload is not a clinical problem as there is loss of iron via hemosiderinuria (*Online Supplementary Figure S1J; Online Supplementary Table S1*). Currently, the patient presents with splenomegaly, but not obvious ophthalmological problems or biliary lithiasis. Overall, the hematological and cytomorphological studies support the diagnosis of CDA type III.

The second patient is a 35-year-old female (Family B, II.1, Figure 1A), with unknown parental consanguinity and a history of antiphospholipid syndrome and papillary thyroid cancer. At birth, she presented with aregenerative macrocytic anemia (*Online Supplementary Table S1*) and significant hepatosplenomegaly. At the age of 5 months, she was diagnosed with CDA III based on bone marrow morphology (Figure 1B). Splenectomy, done at 9 years of age, reduced her transfusion requirements but moderate macrocytic anemia has persisted (hemoglobin [Hb] 96-101 g/L, mean corpuscular volume [MCV] 123 fL). She has short stature and skull defects secondary to increased extramedullary hematopoiesis. Electron microscopy of bone marrow images show irregular heterochromatin and iron-filled mitochondria.[10,11]

A 40-year-old male of Sephardic Jewish descent with the diagnosis of CDA III since childhood (Family C, II.3, Figure 1A), based on bone marrow evaluation, was enrolled in the CDA Registry of North America (CDAR).[12] Family history was negative for anemia; reportedly his parents were second cousins. He was born at full-term and was diagnosed with significant anemia at 4 months of age, requiring transfusion. He continued to receive three to four transfusions per year for a Hb trough <60 g/L up to 24 years of age (*Online Supplementary Table S1*). He had hepatosplenomegaly and skull changes due to bone marrow expansion. Despite deferoxamine infusion subcutaneously 5 nights/week at 12-18 years of age, magnetic resonance imaging (MRI) at 24 years of age showed significant iron overload. Therefore, he was started on a chronic transfusion regimen every 2-4 weeks, with the goal to maintain Hb >100 g/L to suppress ineffective erythropoiesis and on deferoxamine continuous intravenous infusion for 9 months, followed by deferasirox up to 34 years of age when he received hematopoietic stem cell transplant.[13] The patient reports azoospermia discovered at 24 years of age.

Common clinical hematological features in our three reported patients are: macrocytic anemia, aberrant giant multinucleated erythroblasts in the bone marrow and skull defects secondary to severe anemia with ineffective erythropoiesis. Aside from these core features, a clinical variability exists in both *KIF23* and *RACGAP1* patients and a deeper phenotypic characterization will require further cases.

Initially, NGS panels failed to detect pathogenic mutations

in known genes associated with congenital anemia (e.g., *CDAN1*, *CDIN1*, *SEC23B*, *KIF23*, *KLF1* and *GATA1*). In Family A, whole exome sequencing (WES) was performed and predicted pathogenic variants with a minor allele frequency (MAF) <0.03, and proper segregation were selected. *RACGAP1* gene was prioritized as a candidate gene due to its role in cytokinesis and its partnering with MKLP1. A very rare homozygous missense mutation (c.1294C>T;p.Pro432Ser) in *RACGAP1* was found in proband A.II.2 (Figure 1A; *Online Supplementary Figure S1K*). In patient B.II.1, another rare homozygous missense mutation, (c.658A>G;p.Thr220Ala) was found (Figure 1A; *Online Supplementary Figure S1K*). By means of WES in patient C.II.3, the same homozygous p.Thr220Ala mutation was found

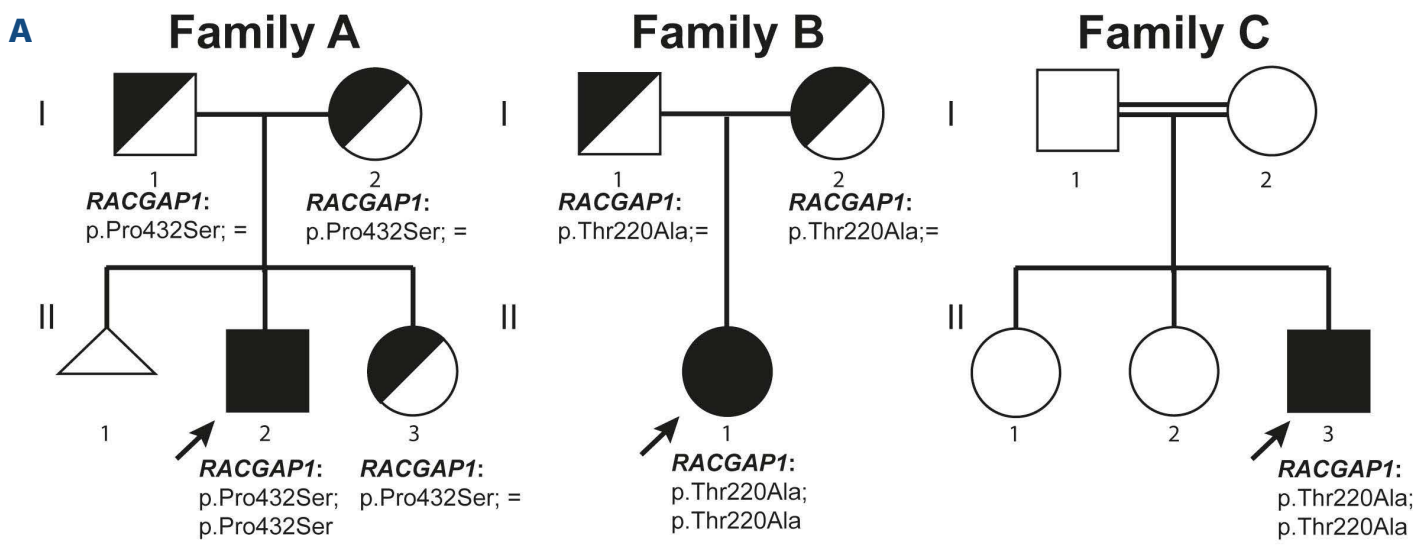

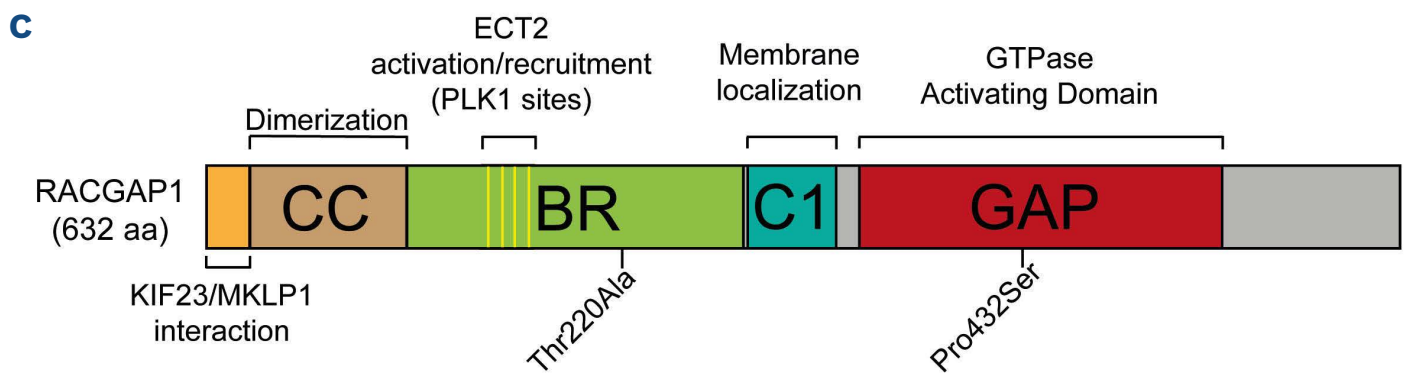

Continued on following page.

Figure 1. *RACGAP1* is mutated in autosomal recessive congenital dyserythropoietic anemia III cases. (A) Pedigrees of the 3 families with affected individuals shown in black and healthy carriers shown in half-filled symbols. The family members shown with white symbols were not tested. RACGAP1 genotypes at the protein level are indicated below each individual. Squares denote males, circles denote females, and triangle denotes pregnancy loss. (B) Bone marrow film images showing a multinucleated erythroid cell (top left), an inter-cytoplasmic chromatin bridge between two multinucleated erythroid cells (top right), a multinucleated erythroid form with karyorrhexis (bottom left) and a giant erythrocyte (bottom right) in patient A.II.2 and multinucleated and dysplastic erythroid progenitors in patient B.II.1. Magnification 100x, scale bars represent 5 µm. Additional images are available in the *Online Supplementary Figure S1* for patient A.II.2. Bone-marrow images from C.II.3 patient are reported elsewhere.[14] (C) Top: schematic representation of RACGAP1 protein domains indicating the localization of the p.Pro432Ser and p.Thr220Ala mutations (CC = coiled-coil, BR = basic region, C1 = cysteine-rich domain, GAP = GTPase-activating domain). Bottom: phylogenetic protein sequence alignment (CLUSTAL omega) of partial RACGAP1 protein sequences showing conservation for Pro432 and Thr220 amino acids. An asterisk (*) denotes fully conserved residue; a colon (:) indicates conservation between amino-acids with strongly similar properties and a period (.) indicates conservation between amino-acids with weakly similar properties.

(*Online Supplementary Figure S1K*). Carrier status for relatives in Family C could not be evaluated as no DNA was available.

p.Pro432Ser and p.Thr220Ala are rare genetic variants (rs760038605 and rs1264268274) with a very low allele frequency (MAF 0.000008 and 0.000004; GnomAD_exomes). Both classified as pathogenic according to ACMG rules (PM2, PP3 and PS3) with CADD scores of 27.3 and 23.4, respectively. Mutations were submitted to ClinVar database (accession number: SCV002540790 and SCV002540791). Pro432 and Thr220 are 100% conserved among vertebrates and are located in the GTPase-activating domain and in the basic region of the RACGAP1 protein, respectively (Figure 1C). The RACGAP1 basic region is required for the interaction with the RHOA–GEF ECT2,[14] among other proteins. Computational modeling of RACGAP1 in complex with RHOA, CDC42, and RAC1 GTPases suggests that the mutation p.Pro432Ser induces local structural changes affecting two RACGAP1 loops involved in complex formation with each of these GTPases (*Online Supplementary Figure S2A*). Modeling of the Thr220Ala mutation is not possible as the crystal structure containing this region of RACGAP1 (or homologous protein) is not available.

Given the erythroid-restricted phenotype associated with CDA III, we investigated by *ex vivo* $CD34^+$ erythroid differentiation whether the identified *RACGAP1* mutations cause alterations like those observed in our patients using flow cytometry and cytospin methods (Figure 2). Both mutations impaired cell growth (data not shown), especially the p.Thr220Ala mutation, therefore, only the erythroid differentiation of A.II.2 patient was fully assessed. At terminal differentiation (day 14), A.II.2-derived-erythrocytes ($CD71^-$;$CD235a^+$ cells) were reduced compared with control cells (Figure 2A, lane 13 and 14). Concomitantly, the number of enucleated cells in cytospins was also reduced (Figure 2B). Lentiviral transduction with wild-type (WT) *RACGAP1* gene restored the erythrocyte population and reduced multinucleated cells enucleating back to control levels at day 14 (Figure 2A, lanes 14 to 16; Figure 2B). This data is supported by cytospin evaluation showing significant multinucleation in *ex vivo* erythropoiesis, which improved after lentiviral transduction of the WT *RACGAP1* gene (Figure 2C to D). Multinucleation defects were also observed in siRNA *RACGAP1*-silenced HeLa cells. Cytokinesis failure was rescued by WT *RACGAP1* construct but not by p.Pro432Ser or p.Thr220Ala mutated *RACGAP1* constructs (*Online Supplementary Figure S2B* to *D*). Importantly, we observed that *ex vivo* erythropoiesis from A.II.2 $CD34^+$ cells phenocopied patient macrocytosis. Lentiviral transduction of WT *RACGAP1* gene also rescued the macrocytic phenotype (Figure 2E and F). Collectively, this data indicates that *RACGAP1* mutations are responsible for the macrocytosis, multinucleation and erythroid defects seen in our patients.

RACGAP1 is a known GTPase regulator required for RHOA activation and for RAC1 inactivation to promote cytokinesis. In patient-derived lymphoblastoid cell lines (LCL) we observed decreased levels of active RHOA and CDC42 GTPases, positive regulators of cytokinesis, and increased levels of active RAC1, an inhibitor of cytokinesis (Figure 3A to C). Our data suggests that *RACGAP1* mutations results in a GTPase imbalance leading to cytokinesis blockage, which could explain the multinucleation defects observed in patient's bone marrow erythroblasts in HeLa cells and in the *ex vivo* $CD34^+$-differentiation.

While preparing this submission, it came to our attention a recent report of a single sporadic case of CDA III with p.Leu396Gln and p.Pro432Ser RACGAP1 mutations, published as a letter to the editor in the Blood journal.[15] The coincidence of the p.Pro432Ser mutation found in both works (Spanish and South American families) may represent a "hot spot" or a founder mutation in the *RACGAP1* gene. The work by Wontakal *et al.*,[15] done independently and in parallel to ours, reinforces our findings and gives some functional data based on HeLa and control erythroid cells. Our work contributes with extensive clinical data in three unrelated patients, detailed characterization of the erythropoiesis defects using patient-derived $CD34^+$ cells, and provides a deeper insight into the molecular mechanisms of these alterations by showing in patient-derived cells a GTPase imbalance that could result in defective cytokinesis.

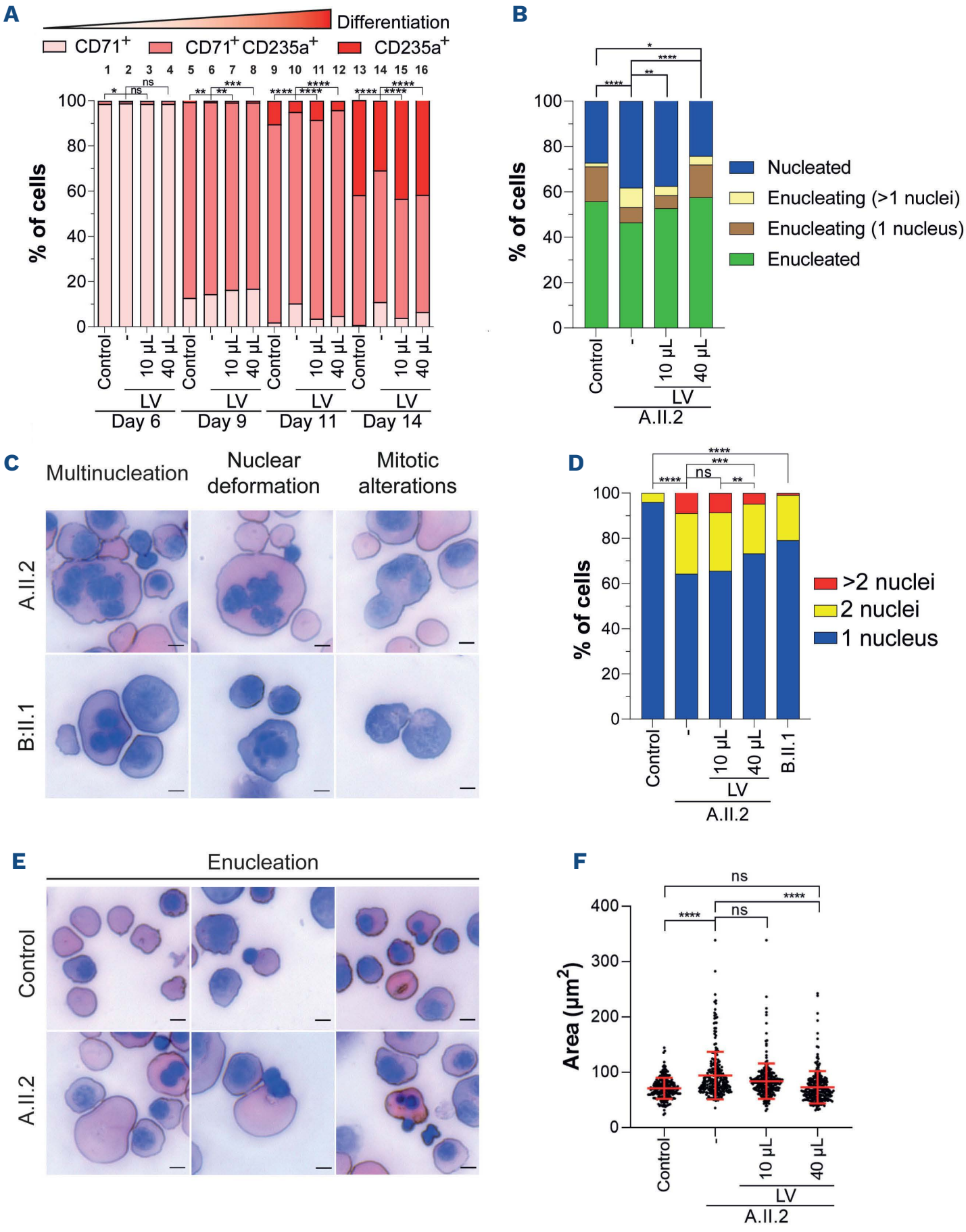

Figure 2. *In vitro* erythroid differentiation of patients' CD34+ cells derived from peripheral blood. (A) Cytometry data of the *in vitro* erythroid differentiation at different time points showing the proportions of erythroid progenitors, erythroblasts, and erythrocytes in the sample (n=1). Results show 10.3% erythrocytes in controls *vs*. 4.9% in A.II.2 cells and 1.92% erythroid progenitors in controls *vs*. 10.3% in A.II.2 cells at day 11 and 41.7% erythrocytes in controls *vs*. 30.7% in A.II.2 cells and 0.79% erythroid progenitors in controls *vs*. 10.96% erythroid progenitors in A.II.2 cells at day 14. Chi-square test with 2 degrees of freedom was performed. (B) Quantification of late erythroblast cells at various stages of the enucleation process in cytospins prepared at day 14. Chi-square test with 3 degrees of freedom was performed (n=484-492). (C) Cytospin preparations stained with modified Wright stain from patients A.II.2 and B.II.1 at day 14 showing multinucleation, nuclear deformations, and mitotic alterations. Scale bars represent 5 µm. (D) Quantification of the percentage of multinucleation at day 14 from the cytospins shown in (C). Chi-square test with 2 degrees of freedom was performed. (E) Cytospin preparations at day 14 showing enucleated cells and cells undergoing enucleation. Scale bars represent 5 µm. (F) Quantification of the area of the enucleated cells from panel (E) showing macrocytosis in the cultures from patient A.II.2's $CD34^+$ cells that is corrected after transduction with the wild-type (WT) *RACGAP1* lentiviral construct (n=252-257). Cell area was calculated using Fiji software by selecting cells using a threshold and watershed separation followed by area determination using the Measure particle program. Due to lack of normality of the data (Kolmogorov-Smirnov test), a Krustal-Wallis test with a Dunn's multiple comparisons test was performed instead of a one-way ANOVA. **P*<0.05, ***P*<0.01, ****P*<0.001, *****P*<0.0001.

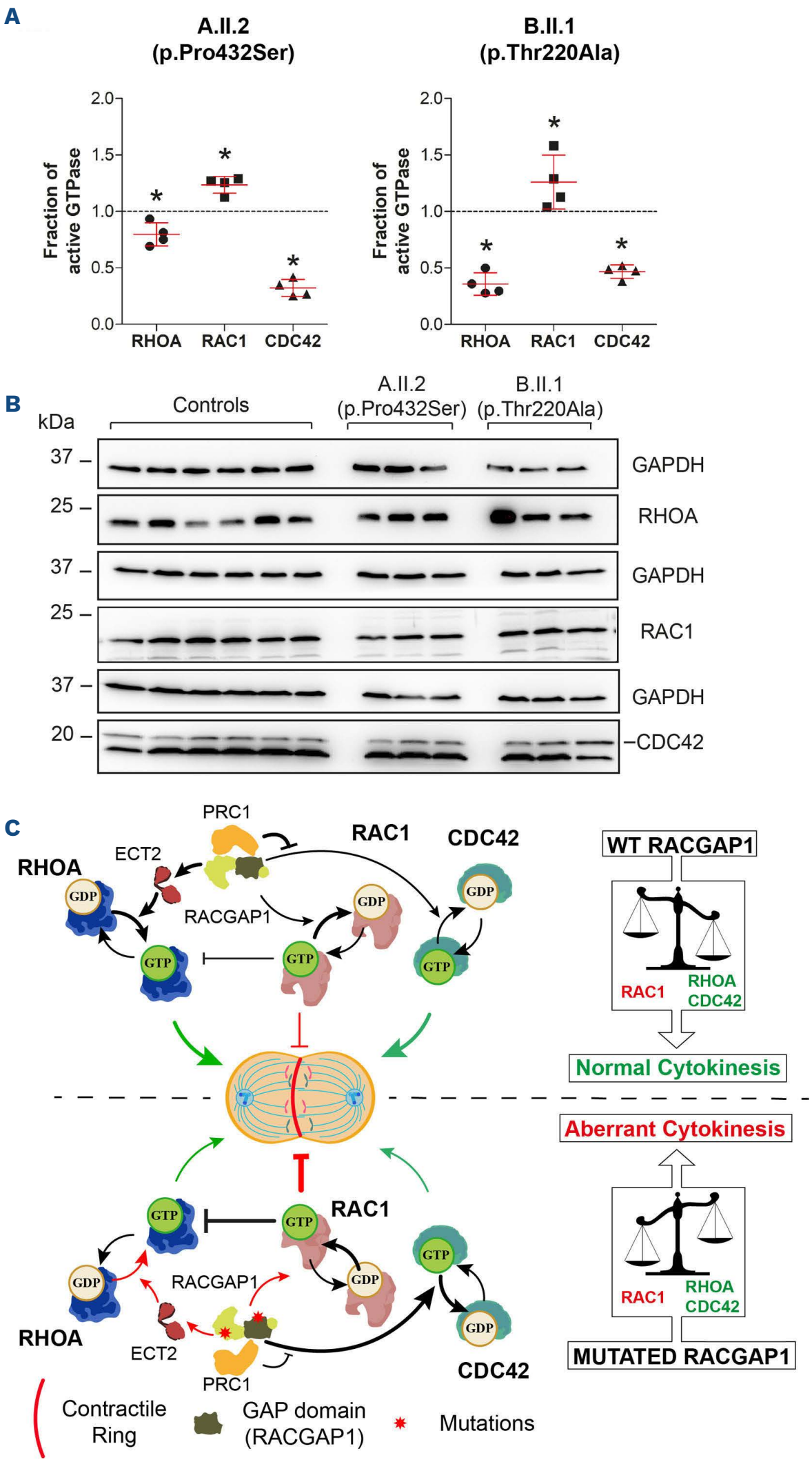

Figure 3. Patients' RACGAP1 mutations alter normal GTPase balance status and model of GTPase regulation in cytokinesis. (A) Amount of active GTPases (RHOA, RAC1 and CDC42) determined by G-LISA in patient-derived lymphoblastoid cell lines (LCL) from A.II.2 and B.II.1 patients normalized to the mean of 2 different controls. G-LISA experiments were done in quadruplicate (n=4). The Mann-Whitney U test was performed to compare GTPase activation levels in each patient with respect to controls. Dotted lines represent the reference of control levels set to 1.0. Error bars represent the mean +/- standard deviation. **P*<0.05, ***P*<0.01, ****P*<0.001. (B) The intermediate step of GTPase activation assessment required for the results shown in (A). Immunoblot of total amounts of RHOA, RAC1 or CDC42 in patients and controls. Three independent protein extracts were generated for each patient/control. The mean amount of each total GTPase was then used to correct the corresponding GTPase activity levels represented in (A). (C) Model for GTPase activation/inactivation in cytokinesis. Correct GTP balance is crucial for cytokinesis. In wild-type (WT) cells (upper panel), RACGAP1 activates RHOA by recruiting the GEF protein ECT2 and directly inactivates RAC1 through its GAP domain, reducing the RAC1-mediated RHOA inhibition. PRC1 inhibits the GAP activity inactivating CDC42. These events generate a strong positive signal to assemble the contractile ring required for cytokinesis. Both mutations (bottom panel) could diminish the RACGAP1-PRC1 interaction, releasing the inhibition to inactivate CDC42. The activation levels of RHOA and CDC42 are diminished while the activation levels of RAC1 are increased, leading to a stronger negative signal towards cytokinesis that leads to a higher degree of multinucleation.

Overall, our work demonstrates that mutations in the *RACGAP1* gene cause a recessively inherited form of CDA III, characterized by moderate to severe anemia due to cytokinesis failures producing multinucleated erythroblast and subsequently ineffective erythropoiesis.

Authors

Gonzalo Hernández,[1,2*] Lídia Romero-Cortadellas,[1*] Xènia Ferrer-Cortès,[1,2] Veronica Venturi,[1] Mercedes Dessy-Rodriguez,[3,4] Mireia

Olivella,[5] Ammar Husami,[6,7] Concepción Pérez de Soto,[8] Rosario M. Morales-Camacho,[9] Ana Villegas,[10] Fernando-Ataulfo González-Fernández,[10] Marta Morado,[11] Theodosia A. Kalfa,[7,12] Oscar Quintana-Bustamante,[3,4] Santiago Pérez-Montero,[2] Cristian Tornador,[2] Jose-Carlos Segovia[3,4] and Mayka Sánchez[1,2]

[1]Department of Basic Sciences, Iron metabolism: Regulation and Diseases Group, Universitat Internacional de Catalunya (UIC), Sant Cugat del Vallès, Spain; [2]BloodGenetics S.L. Diagnostics in Inherited Blood Diseases, Esplugues de Llobregat, Spain; [3]Cell Technology Division, Biomedical Innovative Unit, Centro de Investigaciones Energéticas, Medioambientales y Tecnológicas (CIEMAT) and Centro de Investigación Biomédica en Red de Enfermedades Raras (CIBERER), Madrid, Spain; [4]Unidad Mixta de Terapias Avanzadas, Instituto de Investigación Sanitaria Fundación Jiménez, Madrid, Spain; [5]Bioscience Department, Faculty of Science and Technology (FCT), Universitat de Vic – Universitat Central de Catalunya (Uvic-UCC), Vic, Spain; [6]Division of Human Genetics, Cincinnati Children's Hospital Medical Center, Cincinnati, OH, USA; [7]Department of Pediatrics, University of Cincinnati College of Medicine, Cincinnati, OH USA; [8]Service of Pediatric Hematology, Hospital Universitario Virgen del Rocío, UGC HH, HHUUVR, Sevilla, Spain; [9]Department of Hematology, Hospital Universitario Virgen del Rocío, Instituto de Biomedicina de Sevilla (IBIS/CISC/CIBERONC), Universidad de Sevilla, Sevilla, Spain; [10]Department of Hematology, Hospital Clínico San Carlos. Universidad Complutense, Madrid, Spain; [11]Department of Hematology, Hospital La Paz, Madrid, Spain and [12]Division of Hematology, Cincinnati Children's Hospital Medical Center, Cincinnati, OH, USA

**GH and LR-C contributed equally as co-first authors.*

Correspondence:
M. SÁNCHEZ - msanchezfe@uic.es

https://doi.org/10.3324/haematol.2022.281277

Received: April 29, 2022.
Accepted: September 23, 2022.
Prepublished: October 6, 2022.

Disclosures

No conflicts of interest to disclose.

Contributions

Study concept and research design by MS. Patients' clinical data, blood and bone marrow images by IP-S, R-MM-C, MM, F-AG-F, AV and TAK. Sequencing experiments and mutation validation by XF-C, MS, AH, TAK and CT. WES data analysis by GH, CT, AH, and TAK. Molecular experimental work, data plot and statistical analyses by GH, MD, OQ-B and LR-C. Computational modelling GH and MO. Writing of the manuscript by GH, MS, VV, LR-C and TAK. Funding recruitment by MS, SP-M, J-CS, CT and TAK. All authors participated in data discussion, read, and approved the manuscript.

Acknowledgments

We are very grateful to all families and patients who kindly contributed to this study. We thank Dr Vladimir Benes from European Molecular Biology Laboratory (EMBL), Genomics Core Facility, Heidelberg, Germany for his excellent service in whole exome sequencing. We thank Dr Katie G. Seu and Dr Mary Risinger from Cincinnati Children's Hospital Medical Center for their assistance in proof reading of this manuscript.

Funding

Supported by grant PID2021-122436OB-I00 from MCIN/ AEI /10.13039/501100011033/ ERDF "A way to make Europe" (to MS), PID2020-119637RB-I00 from Ministerio de Ciencia e Innovación y Fondo Europeo de Desarrollo Regional (FEDER)" (to J-CS), AvanCell, B2017/BMD-3692 from Comunidad de Madrid (to J-CS), NEOTEC grant SNEO-20191246 from Spanish CDTI (to CT), grant RTC2019-007074-1 from MCIN/AEI /10.13039/501100011033 (to CT, J-CS and MS), and the U.S. National Heart, Lung, and Blood (NHLBI) Institute grant R01 HL152099 (to TAK). GH is supported by funds provided by the APU and ADISCON Patient associations. LR-C holds an FI-AGAUR predoctoral fellowship (2020FI-B00038) from Generalitat de Catalunya. XF-C is partially supported by funds provided by the grant RTI-2018-101735-B-I100 (MCI/AEI/FEDER, EU). VV was supported by funds provided by APU and ADISCON patient associations and is currently supported by funds provided by UIC postdoctoral scholarship and by funds provided by RETOS COLABORACION grant RTC2019-007074-1 (MCI/AEI/FEDER, EU) from the Spanish Ministry of Science and Innovation (MICINN). J-CS also received funds from Instituto de Investigación Sanitaria "Fundación Jiménez Díaz" and CIBERER, an initiative of the "Instituto de Salud Carlos III" and "Fondo Europeo de Desarrollo Regional (FEDER)".

Data-sharing statement

Data will be shared upon reasonable request.

References

1. Liljeholm M, Irvine AF, Vikberg AL, et al. Congenital dyserythropoietic anemia type III (Cda Iii) is caused by a mutation in kinesin family member, KIF23. Blood. 2013;121(23):4791-4799.
2. Méndez M, Moreno-Carralero MI, Peri VL, et al. Congenital dyserythropoietic anemia types Ib, II, and III: novel variants in the CDIN1 gene and functional study of a novel variant in the KIF23 gene. Ann Hematol. 2021;100(2):353-364.
3. Pavicic-Kaltenbrunner V, Mishima M, Glotzer M. Cooperative assembly of CYK-4/MgcRacGAP and ZEN-4/MKLP1 to form the centralspindlin complex. Mol Biol Cell. 2007;18(12):4992-5003.
4. White EA, Glotzer M. Centralspindlin: at the heart of

cytokinesis. Cytoskeleton. 2012;69(11):882-892.
5. Gambale A, Iolascon A, Andolfo I, Russo R. Diagnosis and management of congenital dyserythropoietic anemias. Expert Rev Hematol. 2016;9(3):283-296.
6. Lind L, Sikstrom C, Sandstrom H, et al. The locus for congenital dyserythropoietic anemia type III (CDA III), associated with monoclonal gammopathy and myeloma, is localized on chromosome 15q21. Am J Hum Genet. 1993;53:A1035.
7. Wickramasinghe SN, Wahlin A, Anstee D, et al. Observations on two members of the Swedish family with congenital dyserythropoietic anaemia, type III. Eur J Haematol. 1993;50(4):213-221.
8. Sandström H, Wahlin A, Eriksson M, Holmgren G, Lind L, Sandgren O. Angioid streaks are part of a familial syndrome of dyserythropoietic anaemia (CDA III). Br J Haematol. 1997;98(4):845-849.
9. Lachowski D, Cortes E, Matellan C, et al. G Protein-coupled estrogen receptor regulates actin cytoskeleton dynamics to impair cell polarization. Front Cell Dev Biol. 2020;8:592628.
10. Villegas A, González L, Furio V, et al. Congenital dyserythropoietic anemia type Iii with unbalanced globin chain synthesis. Eur J Haematol. 1994;52(4):251-253.
11. Pérez-Jacoiste Asín MA, Ruiz Robles G. Skull erythropoiesis in a patient with congenital dyserythropoietic anaemia. Lancet. 2016;387(10020):787.
12. Niss O, Lorsbach RB, Berger M, et al. Congenital dyserythropoietic anemia type I: first report from the Congenital Dyserythropoietic Anemia Registry of North America (CDAR.). Blood Cells Mol Dis. 2021;87:102534.
13. Oh A, Patel PR, Aardsma N, et al. Non-myeloablative allogeneic stem cell transplant with post-transplant cyclophosphamide cures the first adult patient with congenital dyserythropoietic anemia. Bone Marrow Transplant. 2017;52(6):905-906.
14. Petronczki M, Tedeschi A. Cell division: switching on Ect2 in a non-canonical fashion. Curr Biol. 2020;30(16):R947-R949.
15. Wontakal SN, Britto M, Zhang H, et al. RACGAP1 variants in a sporadic case of CDA III implicate the dysfunction of centralspindlin as the basis of the disease. Blood. 2022;139(9):1413-1418.